




# The Siverts asymmetry in charged Kaon and $\Lambda$ hyperon produced SIDIS process at electron ion colliders

Shuailiang Yang<sup>1</sup>, Jianxi Song<sup>1</sup>, Xiaoyu Wang<sup>1,a</sup> , De-Min Li<sup>1,b</sup>, Zhun Lu<sup>2,c</sup>

<sup>1</sup> School of Physics and Microelectronics, Zhengzhou University, Zhengzhou 450001, Henan, China

<sup>2</sup> School of Physics, Southeast University, Nanjing 211189, Jiangsu, China

Received: 7 May 2023 / Accepted: 12 December 2023 / Published online: 18 December 2023  
© The Author(s) 2023

**Abstract** We investigate the single transverse-spin asymmetry with a  $\sin(\phi_h - \phi_S)$  modulation in the charged Kaon produced and in  $\Lambda$  hyperon produced SIDIS process within the theoretical framework of transverse momentum dependent (TMD) factorization at the next-to-leading-logarithmic order. The asymmetry is contributed by the convolution of Siverts function and the unpolarized fragmentation function  $D_1$  for the produced hadron. The parametrization for the proton Qiu–Sterman function, which is closely related to the Siverts function, is adopted to numerically estimate the Siverts asymmetry at the kinematical region of Electron Ion Collider (EIC) and Electron Ion Collider in China (EicC). The TMD evolution of the TMD parton distribution functions are considered by employing the non-perturbative Sudakov form factor. It is found that the predicted Siverts asymmetries  $A_{UT}^{\sin(\phi_h - \phi_S)}$  as functions of  $x$ ,  $z$  and  $P_{hT}$  are sizable at the kinematical configurations of both EIC and EicC. The strange constituent of the produced charged Kaon and  $\Lambda$  hyperon in the final state can be a promising probe of the sea quark Siverts function as well as the flavor dependence in the proton target. Therefore, it is important to utilize the future EIC facilities to constrain the sea quark distribution functions as well as the validity of the generalized universality of the Siverts function.

## 1 Introduction

Since the measurement by the European Muon Collaboration [1, 2] showed that the spin fraction carried by the internal quarks is much smaller than the spin of the proton, which contradicts the conventional theoretical prediction that the constituent quark spin contributes the total proton spin, numer-

ous studies have been carried out to explore the nucleon spin structure from both theoretical and experimental aspects. Among the spin-related observables, the transverse single spin asymmetries (TSSAs) can be the key access to the information of transverse momentum structure of nucleon, which is encoded in the transverse momentum dependent parton distribution functions (TMD PDFs). In leading twist there are eight TMD PDFs, each one describes a distribution of three-dimensional motion of partons with specified polarization inside the nucleon. Particularly, the time-reversal odd (T-odd) Siverts function  $f_{1T}^\perp(x, p_T)$  [3, 4] denotes the asymmetric distribution of unpolarized quarks inside a transversely polarized nucleon, which arises from the correlation between the quark transverse momentum and the nucleon transverse spin. Due to its T-odd property, Siverts function as well as its chiral-odd partner the Boer–Mulders function has been assumed to be forbidden by the naive time-reversal invariance of QCD [5], the very existence of the two T-odd distribution functions was not so obvious. However, the situation has changed since the calculations in Refs. [6–8], which showed that the T-odd distributions can actually survive using spectator model calculations incorporating gluon exchange between the struck quark and the spectator. In Ref. [9], the time-reversal-invariant argument was reexamined and showed the gauge-link in the operator definition of the correlators guarantee the T-odd distribution functions to be nonzero. More importantly, the presence of the gauge-link indicates that Siverts function or the Boer–Mulders function has opposite sign between semi-inclusive deeply inelastic scattering (SIDIS) and Drell–Yan processes [6, 7, 9]

$$f_{1T}^\perp(x, p_T)_{\text{SIDIS}} = -f_{1T}^\perp(x, p_T)_{\text{DY}}, \quad (1)$$

which is a significant prediction by QCD. The verification of the sign change is one of the most fundamental tests of QCD

<sup>a</sup> e-mail: xiaoyuwang@zzu.edu.cn (corresponding author)

<sup>b</sup> e-mail: lidm@zzu.edu.cn

<sup>c</sup> e-mail: zhunlu@seu.edu.cn

prediction, and it is also the main pursue of the existing and future Drell–Yan facilities.

The transverse single spin asymmetry can be utilized to extract the information of the Sivers function, and has been intensively investigated in the past two decades from both experimental and theoretical aspects. The first non-zero Sivers asymmetry was measured by the HERMES Collaboration at DESY in electroproduction of charge pions off the transversely polarized hydrogen target [10]. Updated measurements on the Sivers asymmetry in pion produced as well as those in Kaon and  $p/\bar{p}$  produced in three-dimensional kinematic bin and enlarged phase space were reported in Refs. [11, 12]. The COMPASS Collaboration at CERN also measured the Sivers asymmetries in charged hadrons produced SIDIS process through muon beam scattering off the transversely polarized proton and deuteron targets [13–18]. In addition, the data on the weighted Sivers asymmetry are also released in Ref. [19], allowing for the extractions of the Sivers function and its first transverse moment. The Hall A Collaboration at Jefferson Lab presented the measurement of TSSA in charged pion produced SIDIS process with a transversely polarized  $^3\text{He}$  target [20, 21]. Besides the SIDIS process, COMPASS also measured the Sivers asymmetry in Drell–Yan process via  $\pi N$  collision [22]. Future opportunities will open up at CERN with the LHCspin project [23]. Measurement of TSSAs sensitive to Sivers function in the  $W^\pm$  boson produced in proton–proton collisions has also been performed by the STAR experiments at RHIC [24]. The data from these measurements have been applied to extract the Sivers function using parametrizations and phenomenological approaches [25–36]. Particularly, In Ref. [37], for the first time the 3-dimensional quark density in a fully consistent way within the TMD framework has been utilized to extract the Sivers function, which provide an important parametrization to constrain as well as to cross check the theoretical model calculation and the lattice QCD.

From the theoretical aspect, intensive studies on the quark Sivers function were performed using the QCD-inspired models, such as the spectator model [6, 8, 38]. Then, Ref. [39] separated the diquark spectators into isoscalar ( $ud$ -like) and isovector ( $uu$ -like) spectators to perform the model calculation and obtained all of the leading-twist TMD parton distribution functions. Also the light-cone quark model [40, 41], the light-front quark-diquark model [42, 43], the non-relativistic constituent quark model [44], the MIT bag model [45, 46], and the Holographic QCD [47] have been developed and applied to estimate the valence quark Sivers function. The sea quark Sivers function has been estimated from the light-cone wave function in Refs. [48–50]. However, so far only the valence quark Sivers functions are constrained in the valence region with relatively large uncertainties in the transverse momentum space. One of the reasons is that it is difficult to describe the corresponding physical observ-

ables since there are complicated TMD effects. The TMD evolution effects are encoded in the Sudakov-like form factor which also includes details of the non-perturbative QCD dynamics. Therefore, this part of the Sudakov-like form factor can not be calculated from the perturbative QCD and is mostly unknown. Another reason is that the knowledge of the scale dependence of the TSSAs is very limited since the measurements are mostly performed in the fixed-target experiments with similar hard scales. With the expected high energy and high precision of the Electron Ion Collider (EIC) [51–53] and the Electron Ion Collider in China (EicC) [54, 55], the precise knowledge on the TMD distribution functions may be gained, not only for the valence quarks, but also for sea quarks and gluons. Concerning the sea quark TMDs, the charged Kaon produced or the Lambda hyperon produced in SIDIS can be recognized as an ideal probe to the sea quark distribution of the proton due to the strange constituent quark inside the Kaon and the Lambda hyperon. Therefore, through the Sivers asymmetry in  $K^\pm$  produced and in Lambda produced off transversely polarized nucleon at EIC and EicC, there might be an opportunity to obtain the information of the Sivers distribution function of the sea quark as well as its flavor dependence.

The purpose of this work is to evaluate the Sivers asymmetry in  $ep^\uparrow \rightarrow eK^\pm X$  and in  $ep^\uparrow \rightarrow e\Lambda X$  at the kinematical region of EIC and EicC. The theoretical tool adopted in this study is the TMD factorization formalism [56–59], which has been widely applied to various high energy processes, such as SIDIS [56, 58, 60–66],  $e^+e^-$  annihilation [58, 67, 68], Drell–Yan [58, 64–66, 69, 70], and  $W/Z$  produced in hadron collision [57, 58, 64, 71]. In this framework, the differential cross section can be written as the convolution of the well-defined TMD PDFs and/or fragmentation functions (FFs) at the small transverse momentum region with  $P_{hT}/z \ll Q$  as the constraint to guarantee the TMD factorization validity. The energy dependence of the TMD PDFs and FFs is encoded in the TMD evolution equations, their solutions are usually given in  $b$  space, which is conjugate to the transverse momentum space [57, 58] through Fourier transformation. After solving the TMD evolution equations, the scale dependence of the TMDs may be included in the exponential form of the so-called Sudakov-like form factor [57, 58, 61, 72]. The Sudakov-like form factor can be further separated into perturbatively calculable part and the non-perturbative part, the latter one can not be calculated through perturbative theory and may be obtained by fitting experimental data. We will consider the TMD evolution effects of the corresponding TMDs to obtain the numerical results for the Sivers asymmetry in charged Kaon  $K^\pm$  and  $\Lambda$  hyperon produced SIDIS process.

The rest of the paper is organized as follows. In Sect. 2, we provide the theoretical framework of Sivers asymmetry  $A_{UT}^{\sin(\phi_h - \phi_S)}$  in the charged Kaon produced and  $\Lambda$  hyperon

produced in SIDIS process within the TMD factorization formalism. In Sect. 3, we perform the numerical estimation of the Sivers asymmetry at the kinematical region of EIC and EicC. In Sect. 4, we summarize the work and discuss the results.

### 2 Formalism of the sivers asymmetry in SIDIS process

In this section, we will set up the detailed formalism of the Sivers asymmetry with a modulation of  $\sin(\phi_h - \phi_S)$  in the charged Kaon or Lambda produced SIDIS process with an unpolarized electron beam scattered off a transversely polarized proton target

$$e(\ell) + p(P)^\uparrow \rightarrow e(\ell') + K^\pm/\Lambda(P_h) + X, \tag{2}$$

where  $\ell$  and  $\ell'$  represent the four-momenta of the incoming and outgoing electrons,  $P$  is the four-momentum of the target proton, the up-arrow represents the proton is transversely polarized,  $P_h$  stands for the four-momentum of the final-state hadron, which can be charged Kaon  $K^\pm$  or Lambda hyperon. The four-momentum of the exchanged virtual photon is  $q = \ell - \ell'$  and the usual defined energy scale is  $Q^2 = -q^2$ . We denote the masses of the proton target and the final-state hadron by  $M$  and  $M_h$ . To express the differential cross section as well as the physical observables, we adopt the following Lorentz invariants

$$S = (P + \ell)^2, \quad x = \frac{Q^2}{2P \cdot q}, \quad y = \frac{P \cdot q}{P \cdot \ell}, \quad z = \frac{P \cdot P_h}{P \cdot q}, \tag{3}$$

where  $S$  is the squared center of mass energy,  $x$  represents the Bjorken variable,  $y$  represents the lepton energy momentum transferring fraction, and  $z$  represents the longitudinal momentum fraction of the final fragmented hadron to the parent quark.

The reference frame applied in our study is shown in Fig. 1. According to the Trento convention [73], the  $z$ -axis is defined by the direction of the virtual photon momentum. The azimuthal angle  $\phi_h$  of the outgoing hadron (charged Kaon or Lambda) is defined by

$$\cos \phi_h = -\frac{\ell_\mu P_{h\nu} g_\perp^{\mu\nu}}{\sqrt{\ell_T^2 P_{hT}^2}}, \tag{4}$$

with  $\ell_T^\mu = g_\perp^{\mu\nu} \ell_\nu$  and  $P_{hT}^\mu = g_\perp^{\mu\nu} P_{h\nu}$  being the transverse components of  $\ell$  and  $P_h$  respect to  $z$ -axis. The tensor  $g_\perp^{\mu\nu}$  is

$$g_\perp^{\mu\nu} = g^{\mu\nu} - \frac{q^\mu P^\nu + P^\mu q^\nu}{P(1 + \gamma^2)} + \frac{\gamma^2}{1 + \gamma^2} \left( \frac{q^\mu q^\nu}{Q^2} - \frac{P^\mu P^\nu}{M^2} \right), \tag{5}$$

with  $\gamma = \frac{2Mx}{Q}$ . The azimuthal angle  $\phi_S$  of the proton spin vector  $S$  is defined by replacing  $P_h$  by  $S$  in Eq. (4), and the transverse component of  $S$  is  $S_T^\mu = g_\perp^{\mu\nu} S_\nu$  similar to the definition of  $P_{hT}$ .

Assuming one photon exchange, the model-independent differential cross section can be written as a set of structure functions with the general form as [74]

$$\frac{d\sigma}{dx dy dz d\phi_S d\phi_h dP_{hT}^2} = \frac{\alpha_{em}^2}{xyQ^2} \frac{y}{2(1 - \epsilon)} \left( 1 + \frac{\gamma^2}{2x} \right) \times \left\{ F_{UU,T} + |S_\perp| \sin(\phi_h - \phi_S) F_{UT,T}^{\sin(\phi_h - \phi_S)} + \dots \right\}, \tag{6}$$

where  $F_{UU,T}$  stands for the unpolarized structure function,  $F_{UT,T}^{\sin(\phi_h - \phi_S)}$  is the transverse spin-dependent structure function contributed by the Sivers function,  $\epsilon$  is the ratio of the longitudinal flux and the transverse flux of the photon which has the definition  $\epsilon = \frac{1 - y - \frac{1}{4}\gamma^2 y^2}{1 - y + \frac{1}{2}y^2 + \frac{1}{4}\gamma^2 y^2}$  and the ellipsis denotes other structure functions, which will not be considered in this work. The three subscripts in the structure functions  $F_{XY,Z}$  stand for the polarization of the lepton beam ( $X$ ), the target proton ( $Y$ ) and the virtual photon ( $Z$ ) with U being unpolarized, T being transversely polarized. The Sivers asymmetry is defined as the ratio of the difference between the spin-dependent differential cross sections and the unpolarized differential cross section

$$A_{UT}^{\sin(\phi_h - \phi_S)} \equiv \frac{d\sigma^\uparrow - d\sigma^\downarrow}{d\sigma^\uparrow + d\sigma^\downarrow} = \frac{\sin(\phi_h - \phi_S) F_{UT,T}^{\sin(\phi_h - \phi_S)}}{F_{UU,T}}. \tag{7}$$

The structure functions in Eq. (7) can be expressed as the convolution of the corresponding TMD PDFs and FFs as [74]

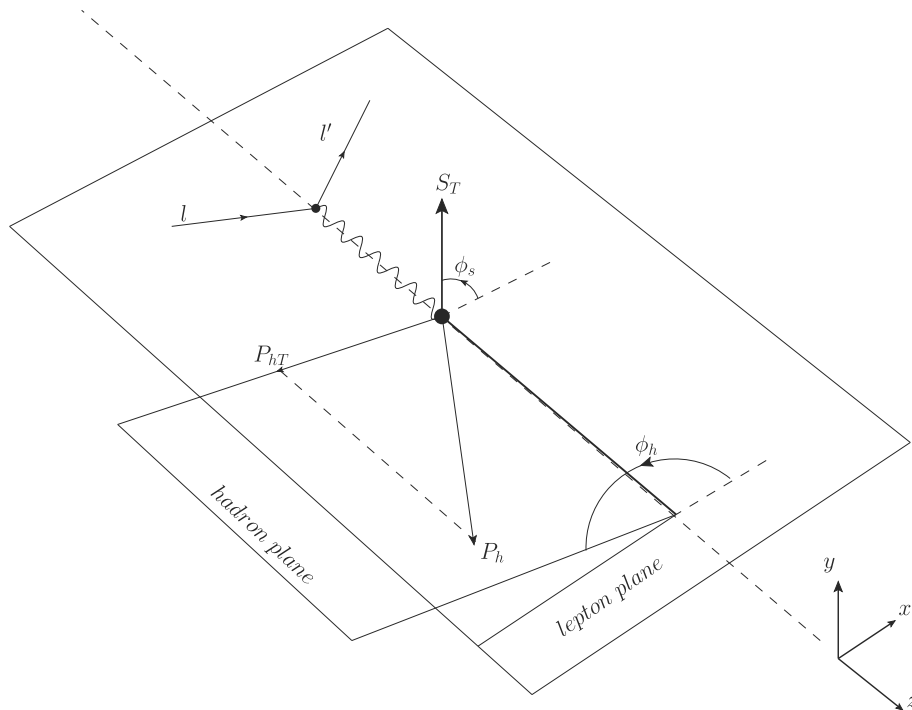
$$F_{UU,T} = \mathcal{C}[f_1 D_1], \tag{8}$$

$$F_{UT,T}^{\sin(\phi_h - \phi_S)} = \mathcal{C} \left[ -\frac{\hat{\mathbf{h}} \cdot \mathbf{p}_T}{M} f_{1T}^\perp D_1 \right]. \tag{9}$$

Here,  $f_1(x, \mathbf{p}_T^2)$  is the unpolarized TMD PDF, and  $f_{1T}^\perp(x, \mathbf{p}_T^2)$  is the Sivers function.  $D_1(z, \mathbf{k}_T^2)$  is the unpolarized TMD FF, which depends on the longitudinal momentum fraction  $z$  and the transverse momentum  $\mathbf{k}_T$  of the final-state quark.  $\hat{\mathbf{h}} = \frac{\mathbf{P}_{hT}}{|\mathbf{P}_{hT}|}$  is the unit vector along  $P_{hT}$ . The notation  $\mathcal{C}$  represents the convolution among the transverse momenta

$$\mathcal{C}[\omega f D] = x \sum_q e_q^2 \int d^2 \mathbf{p}_T d^2 \mathbf{k}_T \delta^{(2)}(\mathbf{p}_T - \mathbf{k}_T - \mathbf{P}_{hT}/z) \times \omega(\mathbf{p}_T, \mathbf{k}_T) f^q(x, \mathbf{p}_T^2) D^q(z, \mathbf{k}_T^2). \tag{10}$$

**Fig. 1** The reference frame in SIDIS process



Substituting Eq. (10) into Eq. (8), we can expand the unpolarized structure function  $F_{UU,T}$  as

$$\begin{aligned}
 F_{UU,T}(Q; P_{hT}) &= C[f_1 D_1] \\
 &= x \sum_q e_q^2 \int d^2 p_T d^2 k_T \delta^{(2)}(p_T - k_T - P_{hT}/z) \\
 &\quad \times f_1^q(x, p_T^2) D_1^q(z, k_T^2) \\
 &= x \sum_q e_q^2 \int d^2 p_T d^2 \frac{K_\perp}{z^2} \delta^{(2)}(p_T + K_\perp/z - P_{hT}/z) \\
 &\quad \times f_1^q(x, p_T^2) D_1^q\left(z, \frac{K_\perp^2}{z^2}\right) \\
 &= x \sum_q e_q^2 \int d^2 p_T d^2 \frac{K_\perp}{z^2} \int \frac{d^2 b}{(2\pi)^2} e^{-i(p_T + K_\perp/z - P_{hT}/z) \cdot b} \\
 &\quad \times f_1^q(x, p_T^2) D_1^q\left(z, \frac{K_\perp^2}{z^2}\right) \\
 &= x \sum_q e_q^2 \int \frac{d^2 b}{(2\pi)^2} e^{i P_{hT} \cdot b/z} \tilde{f}_1^{q/p}(x, b) \tilde{D}_1^{h/q}(z, b),
 \end{aligned} \tag{11}$$

where  $K_\perp$  represents the transverse momentum of the final state hadron with respect to the fragmentation quark, which has the relation  $K_\perp = -z k_T$  with  $k_T$  being the final-state quark transverse momentum respect to  $z$  axis. The  $\delta$ -function Fourier transformation was performed in the fourth line. The TMD distribution function  $\tilde{f}_1(x, b)$  and TMD fragmentation function  $\tilde{D}_1(z, b)$  in the  $b$  space can be obtained by perform-

ing Fourier transformation from momentum space to  $b$  space

$$\begin{aligned}
 \int d^2 p_T e^{-i p_T \cdot b} f_1^q(x, p_T^2) &= \tilde{f}_1^{q/p}(x, b), \tag{12} \\
 \int d^2 \frac{K_\perp}{z^2} e^{-i K_\perp/z \cdot b} D_1^q(z, K_\perp^2) &= \tilde{D}_1^{h/q}(z, b), \tag{13}
 \end{aligned}$$

hereafter, the term with a tilde denotes it is in the  $b$  space. Similarly, substituting Eq. (10) into Eq. (9), we can obtain expansions for the spin-dependent structure function  $F_{UT,T}^{\sin(\phi_h - \phi_s)}$  as

$$\begin{aligned}
 F_{UT,T}^{\sin(\phi_h - \phi_s)}(Q; P_{hT}) &= C \left[ -\frac{\hat{h} \cdot p_T}{M} f_{1T}^\perp D_1 \right] = x \sum_q e_q^2 \int d^2 p_T d^2 k_T \\
 &\delta^{(2)}(p_T + K_\perp/z - P_{hT}/z) \left[ -\frac{\hat{h} \cdot p_T}{M} \right. \\
 &\quad \left. \times f_{1T}^\perp(x, p_T^2) D_1^q(z, k_T^2) \right] \\
 &= x \sum_a e_q^2 \int d^2 p_T d^2 \frac{K_\perp}{z^2} \delta^{(2)}(p_T + K_\perp/z - P_{hT}/z) \\
 &\quad \times \left[ -\frac{\hat{h} \cdot p_T}{M} f_{1T}^\perp(x, p_T^2) D_1^q\left(z, \frac{K_\perp^2}{z^2}\right) \right] \\
 &= x \sum_q e_q^2 \int d^2 p_T d^2 \frac{K_\perp}{z^2} \int \frac{d^2 b}{(2\pi)^2} e^{-i(p_T + K_\perp/z - P_{hT}/z) \cdot b} \\
 &\quad \times \left[ -\frac{\hat{h} \cdot p_T}{M} f_{1T}^\perp(x, p_T^2) D_1^q\left(z, \frac{K_\perp^2}{z^2}\right) \right]
 \end{aligned}$$

$$\begin{aligned}
 &= -\frac{x}{2} \sum_q e_q^2 \int \frac{d^2b}{(2\pi)^2} e^{i\mathbf{p}_{hT} \cdot \mathbf{b}/z} i\hat{\mathbf{h}}_\alpha b^\alpha T_{q,F}(x, x) \\
 &\times \tilde{D}_1^{h/q}(z, b). \tag{14}
 \end{aligned}$$

The Siverts function in  $b$  space can also be obtained from momentum space  $f_1^\perp(x, \mathbf{p}_T^2)$  to  $b$  space by Fourier Transformation as

$$\begin{aligned}
 f_{1T}^{\perp q(\alpha)}(x, b) &= \frac{1}{M} \int d^2p_\perp e^{-i\mathbf{p}_\perp \cdot \mathbf{b}} p_\perp^\alpha f_{1T}^{\perp q}(x, p_\perp^2) \\
 &= \frac{ib^\alpha}{2} T_{q,F}(x, x), \tag{15}
 \end{aligned}$$

where  $\alpha$  is the uncontracted spatial index of the momentum space and  $b$  vectors, the  $T_{q,F}(x, x)$  is the Qiu–Sterman (QS) function. Therefore, the Siverts asymmetry can be rewritten as

$$A_{UT}^{\sin(\phi_h - \phi_s)} = \frac{-\frac{x}{2} \sum_q e_q^2 \int \frac{d^2b}{(2\pi)^2} e^{i\mathbf{p}_{hT} \cdot \mathbf{b}/z} i\hat{\mathbf{h}} \cdot \hat{\mathbf{b}} \sin(\phi_h - \phi_s) T_{q,F}(x, x) \tilde{D}_1^{h/q}(z, b)}{x \sum_q e_q^2 \int \frac{d^2b}{(2\pi)^2} e^{i\mathbf{p}_{hT} \cdot \mathbf{b}/z} \tilde{f}_1^{q/p}(x, b) \tilde{D}_1^{h/q}(z, b)}. \tag{16}$$

One should note that the energy dependence of the TMD structure functions were not encoded in the above formalism, which will be studied in details in the following subsections.

### 2.1 TMD evolution effects

In this subsection, we set up the basic formalism of the TMD evolution effects for TMD PDFs and FFs, which mainly serves to solve the energy dependence of the TMD PDFs  $f_1(x, \mathbf{p}_T^2)$ ,  $f_{1T}^\perp(x, \mathbf{p}_T^2)$  and the TMD FF  $D_1(z, \mathbf{k}_T^2)$ . Since the complicated convolution among the transverse momenta can be transformed into a simple product after performing the Fourier Transformation, it is convenient to solve the energy dependence in  $b$  space.

Particularly, there are two different energy dependencies  $\mu$  and  $\zeta_F$  ( $\zeta_D$ ) of the TMD PDF  $\tilde{F}(x, b)$  and the TMD FF  $\tilde{D}(z, b)$  in  $b$  space according to TMD factorization.  $\mu$  is the renormalization scale related to the corresponding collinear PDFs/FFs, and  $\zeta_F$  ( $\zeta_D$ ) is the energy scale serving as a cutoff to regularize the light-cone singularity in the operator definition of the TMDs. The  $\mu$  and  $\zeta_F$  ( $\zeta_D$ ) dependencies are encoded in different TMD evolution equations. The energy evolution for the  $\zeta_F$  ( $\zeta_D$ ) dependence is encoded in the Collins–Soper (CS) equation[57,58,75]

$$\frac{\partial \ln \tilde{F}(x, b; \mu, \zeta_F)}{\partial \ln \sqrt{\zeta_F}} = \frac{\partial \ln \tilde{D}(z, b; \mu, \zeta_D)}{\partial \ln \sqrt{\zeta_D}} = \tilde{K}(b; \mu), \tag{17}$$

while the  $\mu$  dependence is given by the renormalization group equation

$$\frac{d\tilde{K}}{d \ln \mu} = -\gamma_K(\alpha_s(\mu)), \tag{18}$$

$$\frac{d \ln \tilde{F}(x, b; \mu, \zeta_F)}{d \ln \mu} = \gamma_F\left(\alpha_s(\mu); \frac{\zeta_F^2}{\mu^2}\right), \tag{19}$$

$$\frac{d \ln \tilde{D}(z, b; \mu, \zeta_D)}{d \ln \mu} = \gamma_D\left(\alpha_s(\mu); \frac{\zeta_D^2}{\mu^2}\right), \tag{20}$$

with  $\alpha_s$  being the running strong coupling at the energy scale  $\mu$ ,  $\tilde{K}$  being the CS evolution kernel, and  $\gamma_K$ ,  $\gamma_F$  and  $\gamma_D$  being the anomalous dimensions. Hereafter, we will assume  $\mu = \sqrt{\zeta_F} = \sqrt{\zeta_D} = Q$ , then the TMD PDFs and FFs can be written as  $\tilde{F}(x, b; Q)$  and  $\tilde{D}(z, b; Q)$  for simplicity.

Solving these TMD evolution equations, one can obtain the solution of the energy dependence for TMD parton distribution functions and the fragmentation functions, of which the solution has the general form as

$$\tilde{F}_{q/p}(x, b; Q) = \mathcal{F} \times e^{-S} \times \tilde{F}_{q/p}(x, b; \mu_B), \tag{21}$$

$$\tilde{D}_{h/q}(z, b; Q) = \mathcal{D} \times e^{-S} \times \tilde{D}_{h/q}(z, b; \mu_B), \tag{22}$$

where  $\mathcal{F}$  and  $\mathcal{D}$  is the factor related to the hard scattering and depend on the factorization schemes,  $S$  is the Sudakov-like form factor. Equations (21) and (22) show that the energy evolution of TMD PDFs and TMD fragmentation functions from an initial energy  $\mu_B$  to another energy  $Q$  is encoded in the Sudakov-like form factor  $S$  by the exponential form  $\exp(-S)$ .

By performing the reverse Fourier transformation of the TMDs in  $b$  space, the TMDs in momentum space can be obtained, thus it is of great importance to study the  $b$  space behavior of the TMDs. In the small  $b$  region ( $b \ll 1/\Lambda_{\text{QCD}}$ ), the  $b$  dependence of TMDs is perturbative and can be calculated by perturbative QCD. However, the dependence in large  $b$  region turns to be non-perturbative, since the operators are separated by a large distance. To include the evolution effect in this region, a non-perturbative Sudakov-like form factor  $S_{\text{NP}}$  is introduced and is usually given in a parameterized form. The parameters of  $S_{\text{NP}}$  can be determined by analyzing experimental data, given the lack of non-perturbative calculations. In order to combine the information from both the small  $b$  region and the large  $b$  region, a matching procedure

is applied with a parameter  $b_{\max}$  serving as the boundary between the two regions. Furthermore, one can define a  $b$ -dependent function  $b_*$ , which has the property  $b_* \approx b$  in small  $b$  region and  $b_* \approx b_{\max}$  in large  $b$  region

$$b_* = \frac{b}{\sqrt{1 + b^2/b_{\max}^2}}, \quad b_{\max} < 1/\Lambda_{\text{QCD}}, \quad (23)$$

as given in the original CSS prescription [57]. The prescription also allows for a smooth transition from perturbative to non-perturbative regions and avoids the Landau pole singularity in  $\alpha_s(\mu_B)$ . The typical value of  $b_{\max}$  is chosen around  $1.5 \text{ GeV}^{-1}$  to guarantee that  $b_*$  is always in the perturbative region. With the constraint of  $b_*$ , we can calculate TMDs within a small  $b$  region. While, one should notice that, although the original CSS prescription can provide an effective way to perform the calculation at small  $b$  region, there can be an issue at very small  $b \rightarrow 0$  region, the value of  $\mu_B$  may be larger than  $Q$ , which will lead to problems of Fourier Transformation as well as the computation of Sudakov form factor. It can be resolved by introducing the lower limit of  $b_*$  [64, 66, 70].

In the small  $b$  region, the TMDs can be expressed as the convolutions of the perturbatively calculable hard coefficients and the corresponding collinear counterparts at fixed energy  $\mu_B$ , which could be the collinear PDFs/FFs or the multiparton correlation functions [56, 76]

$$\tilde{F}_{q/p}(x, b; \mu_B) = C_{q \leftarrow i} \otimes F_{i/p}(x, \mu_B), \quad (24)$$

$$\tilde{D}_{h/q}(z, b; \mu_B) = \hat{C}_{j \leftarrow q} \otimes D_{h/j}(z, \mu_B), \quad (25)$$

where  $\mu_B = c_0/b_*$  and  $c_0 = 2e^{-\gamma_E}$  and the Euler constant  $\gamma_E \approx 0.577$  [56], the  $\otimes$  stands for the convolution in the momentum fraction  $x$

$$C_{q \leftarrow i} \otimes F_{i/p}(x, \mu_B) \equiv \sum_i \int_x^1 \frac{d\xi}{\xi} C_{q \leftarrow i} \times \left(\frac{x}{\xi}, \mu_B\right) F_{i/p}(\xi, \mu_B), \quad (26)$$

$$\hat{C}_{j \leftarrow q} \otimes D_{h/j}(z, \mu_B) \equiv \sum_j \int_z^1 \frac{d\xi}{\xi} \hat{C}_{j \leftarrow q} \times \left(\frac{z}{\xi}, \mu_B\right) D_{h/j}(\xi, \mu_B), \quad (27)$$

where  $C$  coefficients in the formula has different values in different processes, and its specific value will be given in the subsequent calculation. In addition, the sum  $\sum_i$  runs over all parton flavors. Now we can combine all the above information to get the expression for TMD distribution function and the fragmentation function in  $b$  space as

$$\begin{aligned} \tilde{F}_{q/p}(x, b; Q) &= \mathcal{F} \times e^{-S} \times C_{q \leftarrow i} \otimes F_{i/p}(x, \mu_B) \\ &= \mathcal{F} \times e^{-S} \times \sum_i \int_x^1 \frac{d\xi}{\xi} C_{q \leftarrow i} \left(\frac{x}{\xi}, \mu_B\right) \\ &\quad \times F_{i/p}(\xi, \mu_B), \end{aligned} \quad (28)$$

$$\begin{aligned} \tilde{D}_{h/q}(z, b; Q) &= \mathcal{D} \times e^{-S} \times \hat{C}_{j \leftarrow i} \otimes D_{h/j}(z, \mu_B) \\ &= \mathcal{D} \times e^{-S} \times \sum_j \int_z^1 \frac{d\xi}{\xi} \hat{C}_{j \leftarrow q} \left(\frac{z}{\xi}, \mu_B\right) \\ &\quad \times D_{h/j}(\xi, \mu_B). \end{aligned} \quad (29)$$

The Sudakov-like form factor  $S$  can be separated into the perturbatively calculable part  $S_{\text{pert}}(Q; b_*)$  and the non-perturbative part  $S_{\text{NP}}(Q; b)$

$$S(Q; b) = S_{\text{pert}}(Q; b_*) + S_{\text{NP}}(Q; b). \quad (30)$$

The perturbative part  $S_{\text{pert}}(Q; b_*)$  has a general form and can be expanded as the series of  $(\frac{\alpha_s}{\pi})$  [32, 63, 77–79].

$$S_{\text{pert}}(Q; b_*) = \int_{\mu_B^2}^{Q^2} \frac{d\bar{\mu}^2}{\bar{\mu}^2} \left[ A(\alpha_s(\bar{\mu})) \ln\left(\frac{Q^2}{\bar{\mu}^2}\right) + B(\alpha_s(\bar{\mu})) \right]. \quad (31)$$

Also the coefficients  $A$  and  $B$  can be expanded as following

$$A = \sum_{n=1}^{\infty} A^{(n)} \left(\frac{\alpha_s}{\pi}\right)^n, \quad (32)$$

$$B = \sum_{n=1}^{\infty} B^{(n)} \left(\frac{\alpha_s}{\pi}\right)^n. \quad (33)$$

In our calculation we take  $A^{(n)}$  up to  $A^{(2)}$  and  $B^{(n)}$  up to  $B^{(1)}$  [57, 61, 63, 77, 80, 81],

$$A^{(1)} = C_F, \quad (34)$$

$$A^{(2)} = \frac{C_F}{2} \left[ C_A \left(\frac{67}{18} - \frac{\pi^2}{6}\right) - \frac{10}{9} T_R n_f \right], \quad (35)$$

$$B^{(1)} = -\frac{3}{2} C_F. \quad (36)$$

For the non-perturbative Sudakov-like form factor  $S_{\text{NP}}(Q; b)$ , it cannot be obtained from perturbation calculation, and it is usually extracted from the experimental data. Inspired by Refs. [80, 82], a widely used Gaussian form parametrization of  $S_{\text{NP}}$  for TMD PDFs or fragmentation functions was proposed [32, 64, 66, 70, 76, 80, 82–84]

$$S_{\text{NP}}^{\text{pdf/ff}} = b^2 \left( g_1^{\text{pdf/ff}} + \frac{g_2}{2} \ln \frac{Q}{Q_0} \right), \quad (37)$$

where the initial energy is  $Q_0^2 = 2.4 \text{ GeV}^2$ , and the factor  $1/2$  in front of  $g_2$  comes from the fact that only one hadron is involved for the parametrization of  $S_{\text{NP}}^{\text{pdf/ff}}$ . The parameter  $g_1^{\text{pdf/ff}}$  in Eq. (37) depends on the type of TMDs, which can be regarded as the width of the intrinsic transverse momentum for the relevant TMDs at the initial energy scale  $Q_0$  [30, 61, 81]. Assuming a Gaussian form with a constant width for the dependence on the transverse momentum, we obtain

$$g_1^{\text{pdf}} = \frac{\langle p_{\perp}^2 \rangle_{Q_0}}{4}, \quad g_1^{\text{ff}} = \frac{\langle k_{\perp}^2 \rangle_{Q_0}}{4z^2}, \tag{38}$$

where  $\langle p_{\perp}^2 \rangle_{Q_0}$  and  $\langle k_{\perp}^2 \rangle_{Q_0}$  represent the averaged intrinsic transverse momenta squared for TMD PDFs and FFs at the initial scale  $Q_0$ , respectively. The value of  $g_2$  is different in the different TMD analyses, here we follow Ref. [32] to choose  $g_2 = 0.16$ .

As the information on the Sudakov-like form factor for the Kaon fragmentation functions can not be determined, we assume that the evolution of the TMD distribution function and the fragmentation function for producing the  $K$  meson from the initial energy scale  $\mu$  to another energy scale  $Q$  follows the Gaussian form of  $g_2(b)$  in Eq. (37), so we can obtain the non-perturbative Sudakov-like form factor for the PDF and FF for the production of the  $K$  mesons as

$$S_{\text{NP}}^{\text{pdf}}(Q; b) = \frac{g_2}{2} \ln\left(\frac{Q}{Q_0}\right) b^2 + g_1^{\text{pdf}} b^2, \tag{39}$$

$$S_{\text{NP}}^{\text{ff}}(Q; b) = \frac{g_2}{2} \ln\left(\frac{Q}{Q_0}\right) b^2 + g_1^{\text{ff}} b^2. \tag{40}$$

Combining all the steps mentioned above together, the scale-dependent TMD PDFs and FFs in  $b$  space as functions of  $x$  (or  $z$ ),  $b$ , and  $Q$  can be rewritten as

$$\begin{aligned} \tilde{F}_{q/p}(x, b; Q) &= e^{-\frac{1}{2}S_{\text{Pert}}(Q; b_*) - S_{\text{NP}}^{\text{pdf}}(Q; b)} \mathcal{F}(\alpha_s(Q)) \\ &\times \sum_i \int_x^1 \frac{d\xi}{\xi} C_{q \leftarrow i}\left(\frac{x}{\xi}, \mu_B\right) F_{i/p}(\xi, \mu_B), \end{aligned} \tag{41}$$

$$\begin{aligned} \tilde{D}_{h/q}(z, b; Q) &= e^{-\frac{1}{2}S_{\text{Pert}}(Q; b_*) - S_{\text{NP}}^{\text{ff}}(Q; b)} \mathcal{D}(\alpha_s(Q)) \\ &\times \sum_j \int_z^1 \frac{d\xi}{\xi} \hat{C}_{j \leftarrow q}\left(\frac{z}{\xi}, \mu_B\right) D_{h/j}(\xi, \mu_B). \end{aligned} \tag{42}$$

### 2.2 The solution of the unpolarized structure function

In the following we solve the denominator of the Siverson asymmetry in details, which is the unpolarized structure function  $F_{UU,T}$  in Eq. (8). Since we have expanded  $F_{UU,T}$  in Eq. (11), we will directly follow Eq. (11) to give the complete expression for  $F_{UU,T}$ . According to Eqs. (41) and (42),  $\tilde{f}_1^q(x, b)$

and  $\tilde{D}_1^{h/q}(z, b)$  can be expanded as

$$\begin{aligned} \tilde{f}_1^{q/p}(x, b; Q) &= e^{-\frac{1}{2}S_{\text{Pert}}(Q; b_*) - S_{\text{NP}}^{f_1}(Q; b)} \mathcal{F}(\alpha_s(Q)) \\ &\times \sum_i \int_x^1 \frac{d\xi}{\xi} C_{q \leftarrow i}\left(\frac{x}{\xi}, \mu_B\right) f_1^{i/p}(\xi, \mu_B), \end{aligned} \tag{43}$$

$$\begin{aligned} \tilde{D}_1^{h/q}(z, b; Q) &= e^{-\frac{1}{2}S_{\text{Pert}}(Q; b_*) - S_{\text{NP}}^{D_1}(Q; b)} \mathcal{D}(\alpha_s(Q)) \\ &\times \sum_j \int_z^1 \frac{d\xi}{\xi} \hat{C}_{j \leftarrow q}\left(\frac{z}{\xi}, \mu_B\right) D_1^{h/j}(\xi, \mu_B), \end{aligned} \tag{44}$$

substituting Eqs. (43) and (44) into the unpolarized structure function in Eq. (8), one can have the following expression

$$\begin{aligned} F_{UU,T}(Q; P_{hT}) &= x \int \frac{d^2b}{(2\pi)^2} e^{iP_{hT} \cdot b/z} \tilde{F}_{UU,T}(Q; b) \\ &= x \int_0^\infty \frac{dbb}{2\pi} J_0\left(\frac{P_{hT}b}{z}\right) \tilde{F}_{UU,T}(Q; b), \end{aligned} \tag{45}$$

where  $J_0\left(\frac{P_{hT}b}{z}\right)$  represents the Bessel function,  $\tilde{F}_{UU,T}(Q; b)$  has the expression as

$$\begin{aligned} \tilde{F}_{UU,T}(Q; b) &= e^{-S_{\text{pert}}(Q; b_*) - S_{\text{NP}}^{\text{SIDIS}}(Q; b)} \sum_q e_q^2 \mathcal{F}(\alpha_s(Q)) \mathcal{D}(\alpha_s(Q)) \\ &\times \left( \sum_i \int_x^1 \frac{d\xi}{\xi} C_{q \leftarrow i}^{(\text{SIDIS})}\left(\frac{x}{\xi}, \mu_B\right) f_1^{i/p}(\xi, \mu_B) \right) \\ &\times \left( \sum_j \int_z^1 \frac{d\xi}{\xi} \hat{C}_{j \leftarrow q}^{(\text{SIDIS})}\left(\frac{z}{\xi}, \mu_B\right) D_1^{h/j}(\xi, \mu_B) \right), \end{aligned} \tag{46}$$

where the Sudakov-like form factor is expressed in Eqs. (31), (39) and (40). The hard scattering coefficients  $\mathcal{F}(\alpha_s(Q))$  and  $\mathcal{D}(\alpha_s(Q))$  can be set equal to 1. In addition, the  $C$  and  $\hat{C}$  coefficient in Eqs. (43) and (44) can be expressed as [85]

$$\begin{aligned} C_{q \leftarrow q'}^{(\text{SIDIS})}(x, \mu_B) &= \delta_{q'q} \left[ \delta(1-x) + \frac{\alpha_s}{\pi} \left( \frac{C_F}{2} (1-x) \right. \right. \\ &\quad \left. \left. - 2C_F \delta(1-x) \right) \right], \end{aligned} \tag{47}$$

$$C_{q \leftarrow g}^{(\text{SIDIS})}(x, \mu_B) = \frac{\alpha_s}{\pi} T_R x(1-x), \tag{48}$$

$$\begin{aligned} \hat{C}_{q' \leftarrow q}^{(\text{SIDIS})}(z, \mu_B) &= \delta_{q'q} \left[ \delta(1-z) + \frac{\alpha_s}{\pi} \left( \frac{C_F}{2} (1-z) \right. \right. \\ &\quad \left. \left. - 2C_F \delta(1-z) + P_{q \leftarrow q}(z) \ln z \right) \right], \end{aligned} \tag{49}$$

$$\hat{C}_{g \leftarrow q}^{(\text{SIDIS})}(z, \mu_B) = \frac{\alpha_s}{\pi} \left( \frac{C_F}{2} z + P_{g \leftarrow q}(z) \ln z \right), \tag{50}$$

where  $\alpha_s$  represents the strong coupling, and the expansion at the next-to-leading order can be written as follows

$$\alpha_s(Q^2) = \frac{12\pi}{(33 - 2n_f) \ln(Q^2/\Lambda_{QCD}^2)} \times \left\{ 1 - \frac{6(153 - 19n_f) \ln \ln(Q^2/\Lambda_{QCD}^2)}{(33 - 2n_f)^2 \ln(Q^2/\Lambda_{QCD}^2)} \right\}. \tag{51}$$

In Eq. (51),  $Q^2$  is the running energy scale and  $n_f = 5$ ,  $\Lambda_{QCD} = 0.225$  GeV. The splitting functions  $P_{q \leftarrow q}$  and  $P_{g \leftarrow q}$  in Eqs. (49) and (50) have the general form

$$P_{q \leftarrow q}(z) = C_F \left[ \frac{1 + z^2}{(1 - z)_+} + \frac{3}{2} \delta(1 - z) \right], \tag{52}$$

$$P_{g \leftarrow q}(z) = C_F \frac{1 + (1 - z)^2}{z}, \tag{53}$$

where  $C_F = 4/3$ ,  $T_R = 1/2$ , and the subscript symbol “+” denotes the following prescription

$$\int_0^1 dz \frac{f(z)}{(1 - z)_+} = \int_0^1 dz \frac{f(z) - f(1)}{(1 - z)}. \tag{54}$$

Combining the above information, we can obtain the final expression of the unpolarized structure function  $F_{UU,T}(Q; P_{hT})$  as follows

$$\begin{aligned} &F_{UU,T}(Q; P_{hT}) \\ &= x \sum_q e_q^2 \int_0^\infty \frac{bdb}{(2\pi)} J_0\left(\frac{P_{hT}b}{z}\right) e^{-S_{\text{pert}}(Q;b_*) - S_{\text{NP}}^{\text{SIDIS}}(Q;b)} \\ &\times \left( \sum_i \int_x^1 \frac{d\xi}{\xi} C_{q \leftarrow i}^{\text{SIDIS}}\left(\frac{x}{\xi}, \mu_B\right) f_1^{i/p}(\xi, \mu_B) \right) \\ &\times \left( \sum_j \int_z^1 \frac{d\xi}{\xi} \hat{C}_{j \leftarrow q}^{\text{SIDIS}}\left(\frac{z}{\xi}, \mu_B\right) D_1^{h/j}(\xi, \mu_B) \right), \tag{55} \end{aligned}$$

where the non-perturbative Sudakov-like form factor  $S_{\text{NP}}^{\text{SIDIS}}(Q; b)$  receives the contribution from the unpolarized TMD PDF and FF:

$$\begin{aligned} S_{\text{NP}}^{\text{SIDIS}}(Q; b) &= S_{\text{NP}}^{\text{f}_1}(Q; b) + S_{\text{NP}}^{\text{D}_1}(Q; b) \\ &= g_2 \ln\left(\frac{Q}{Q_0}\right) b^2 + g_1^{\text{f}_1} b^2 + g_1^{\text{D}_1} b^2. \tag{56} \end{aligned}$$

Here,  $g_1^{\text{f}_1}$  and  $g_1^{\text{D}_1}$  are obtained from Eq. (38), so  $g_1^{\text{f}_1} = g_1^{\text{pdf}} = \frac{\langle p_\perp^2 \rangle_{Q_0}}{4}$ ,  $g_1^{\text{D}_1} = g_1^{\text{ff}} = \frac{\langle k_\perp^2 \rangle_{Q_0}}{4z^2}$ .

### 2.3 The solution of the transverse spin-dependent structure function

Similar to the previous subsection, we further obtain the expression for the transverse spin-dependent structure function  $F_{UT,T}^{\sin(\phi_h - \phi_s)}$ . We have initially expanded  $F_{UT,T}^{\sin(\phi_h - \phi_s)}$  in Eq. (14), we will directly follow Eq. (14) to give the complete expression for  $F_{UT,T}^{\sin(\phi_h - \phi_s)}$ . According to Eq. (41), the QS function  $T_{q,F}(x', x'')$  in the  $b$  space has a similar solution form after solving the TMD evolution equations

$$T_{q,F}(x, x; Q) = T \times e^{-S} \times T_{q,F}(x, x; \mu_B), \tag{57}$$

In the small  $b$  region, the QS function can be calculated from the convolution of the hard scattering coefficients and the collinear counterpart utilizing the perturbative QCD

$$T_{q,F}(x, x; \mu_B) = \Delta C_{q \leftarrow i}^T \otimes T_{i,F}(x, x; \mu_B), \tag{58}$$

where  $\otimes$  denotes convolution and can be expanded as

$$\begin{aligned} &\Delta C_{q \leftarrow i}^T \otimes T_{i,F}(x, x; \mu_B) \\ &= \sum_i \int_x^1 \frac{d\xi}{\xi} \Delta C_{q \leftarrow i}^T\left(\frac{x}{\xi}, \mu_B\right) T_{i,F}(\xi, \xi; \mu_B), \tag{59} \end{aligned}$$

substituting Eq. (59) into Eq. (58), we can obtain the expansion of the QS function  $T_{q,F}(x', x'')$  as

$$\begin{aligned} T_{q,F}(x, x; Q) &= e^{-\frac{1}{2} S_{\text{pert}}(Q;b_*) - S_{\text{NP}}^{\text{f}_1}(Q;b)} \mathcal{T}(\alpha_s(Q)) \\ &\times \sum_i \int_x^1 \frac{d\xi}{\xi} \Delta C_{q \leftarrow i}^T\left(\frac{x}{\xi}, \mu_B\right) \\ &\times T_{i,F}(\xi, \xi; \mu_B). \tag{60} \end{aligned}$$

In addition, the expansions of the fragmentation function  $\tilde{D}_1^{h/q}(z, b)$  can be obtained from Eq. (44) as

$$\begin{aligned} \tilde{D}_1^{h/q}(z, b; Q) &= e^{-\frac{1}{2} S_{\text{pert}}(Q;b_*) - S_{\text{NP}}^{\text{D}_1}(Q;b)} \mathcal{D}(\alpha_s(Q)) \\ &\times \sum_j \int_z^1 \frac{d\xi}{\xi} \hat{C}_{j \leftarrow q}\left(\frac{z}{\xi}, \mu_B\right) D_1^{h/j}(\xi, \mu_B), \tag{61} \end{aligned}$$

substituting Eqs. (60) and (61) into the transverse spin-dependent structure function in Eq. (14), one can have

$$\begin{aligned} &F_{UT,T}^{\sin(\phi_h - \phi_s)}(Q; P_{hT}) \\ &= -\frac{x}{2} \int \frac{d^2b}{(2\pi)^2} e^{i P_{hT} \cdot b/z} i \hat{h}_\alpha b^\alpha \tilde{F}_{UT,T}(Q; b) \\ &= \frac{x}{2} \int_0^\infty \frac{b^2 db}{2\pi} J_1\left(\frac{P_{hT}b}{z}\right) \tilde{F}_{UT,T}(Q; b), \tag{62} \end{aligned}$$



the structure function  $\tilde{F}_{UT,T}(Q; b)$  can be expanded into

$$\begin{aligned} &\tilde{F}_{UT,T}(Q; b) \\ &= e^{-S_{\text{pert}}(Q; b_*) - S_{\text{NP}}^{\text{SIDIS}}(Q; b)} \sum_q e_q^2 \mathcal{T}(\alpha_s(Q)) \mathcal{D}(\alpha_s(Q)) \\ &\quad \times \left( \sum_i \int_x^1 \frac{d\xi}{\xi} \Delta C_{q \leftarrow i}^{T(DIS)} \left( \frac{x}{\xi}, \mu_B \right) T_{i,F}(\xi, \xi; \mu_B) \right) \\ &\quad \times \left( \sum_j \int_z^1 \frac{d\xi}{\xi} \hat{C}_{j \leftarrow q}^{(SIDIS)} \left( \frac{z}{\xi}, \mu_B \right) D_1^{h/j}(\xi, \mu_B) \right), \end{aligned} \tag{63}$$

where the Sudakov-like form factor is expressed in Eqs. (31), (39) and (40). And the hard scattering coefficient  $\mathcal{T}(\alpha_s(Q))$  and  $\mathcal{D}(\alpha_s(Q))$  equal to 1. The  $\hat{C}$  coefficient of  $\tilde{D}_1^q(z, b)$  is expressed in Eqs. (49), (50), (52) and (53). The expression of  $\Delta C$  in Eq. (60) is [86]

$$\begin{aligned} &\Delta C_{qq}^{T(DIS)}(x, \mu_B) \\ &= \delta(1-x) + \frac{\alpha_s(\mu_B)}{\pi} \left( -\frac{1}{4N_c}(1-x) - 2C_F\delta(1-x) \right), \end{aligned} \tag{64}$$

where  $N_c = 3$ . Combining the above information, we can obtain the final expression of the transverse spin-dependent structure function  $F_{UT,T}^{\sin(\phi_h - \phi_s)}$  as follows

$$\begin{aligned} &F_{UT,T}^{\sin(\phi_h - \phi_s)} \\ &= \frac{x}{2} \sum_q e_q^2 \int_0^\infty \frac{b^2 db}{2\pi} J_1\left(\frac{P_{hT} b}{z}\right) e^{-S_{\text{pert}}(Q; b_*) - S_{\text{NP}}^{\text{SIDIS}}(Q; b)} \\ &\quad \times \left( \sum_i \int_x^1 \frac{d\xi}{\xi} \Delta C_{q \leftarrow i}^{T(DIS)} \left( \frac{x}{\xi}, \mu_B \right) T_{i,F}(\xi, \xi; \mu_B) \right) \\ &\quad \times \left( \sum_j \int_z^1 \frac{d\xi}{\xi} \hat{C}_{j \leftarrow q}^{(SIDIS)} \left( \frac{z}{\xi}, \mu_B \right) D_1^{h/j}(\xi, \mu_B) \right), \end{aligned} \tag{65}$$

where the non-perturbative Sudakov-like form factor  $S_{\text{NP}}^{\text{SIDIS}}(Q; b)$  is the combination of the one for the Sivvers function and the one for the unpolarized TMD FF

$$\begin{aligned} &S_{\text{NP}}^{\text{SIDIS}}(Q; b) = S_{\text{NP}}^{\text{Sivvers}}(Q; b) + S_{\text{NP}}^{\text{D1}}(Q; b) \\ &= g_2 \ln\left(\frac{Q}{Q_0}\right) b^2 + g_1^{\text{Sivvers}} b^2 + g_1^{\text{D1}} b^2, \end{aligned} \tag{66}$$

where  $g_1^{\text{Sivvers}} = \frac{\langle k_{s\perp}^2 \rangle}{4}$ ,  $g_1^{\text{D1}} = \frac{\langle k_{1\perp}^2 \rangle_{Q_0}}{4z^2}$ .

### 3 Numerical estimate

In this section, we present the numerical estimate for the Sivvers asymmetry in charged Kaon and  $\Lambda$  hyperon produced SIDIS process at the kinematical configurations of EIC and EicC.

In order to obtain the results for the Sivvers asymmetry, we shall have the collinear distribution functions and fragmentation functions as input. For the unpolarized proton collinear distribution function  $f_1(x, \mu_B)$ , we apply the parametrization from MSTW2008 [87]. For the collinear unpolarized fragmentation function  $D_1(z)$  of charged Kaon, the DSS parameterization results at LO accuracy is used [88]. For the collinear unpolarized fragmentation function  $D_1^\Lambda(z)$  of  $\Lambda$  hyperon, we adopt the model results from the diquark spectator model [89]

$$\begin{aligned} &D_1^\Lambda(z) = \frac{g_s^2}{4(2\pi)^2} \frac{e^{-\frac{2m_q^2}{\Lambda^2}}}{z^4 L^2} \left\{ z(1-z) \left( (m_q + M_\Lambda)^2 - m_D^2 \right) \right. \\ &\quad \times \exp\left(\frac{-2zL^2}{(1-z)\Lambda^2}\right) \\ &\quad + \left. \left( (1-z)\Lambda^2 - 2((m_q + M_\Lambda)^2 - m_D^2) \right) \right. \\ &\quad \times \left. \frac{z^2 L^2}{\Lambda^2} \Gamma\left(0, \frac{2zL^2}{(1-z)\Lambda^2}\right) \right\}. \end{aligned} \tag{67}$$

The values of the free parameters in Eq. (67) are taken from Ref. [89]. Since the model result is obtained at the initial energy of 0.23 GeV<sup>2</sup>, to make it applicable to a more general energy range, we use the QCDNUM evolution package [90] to evolve the unpolarized fragmentation function  $D_1(z)$  from the initial energy of 0.23 GeV<sup>2</sup> to another energy scale.

For the Qiu–Sterman (QS) function  $T_{q,F}(x, x; \mu_B)$ , we adopt the extraction from the parameterization in Ref. [32]

$$\begin{aligned} &T_{q,F}(x, x, \mu_B) = N_q \frac{(\alpha_q + \beta_q)^{(\alpha_q + \beta_q)}}{\alpha_q^{\alpha_q} \beta_q^{\beta_q}} x^{\alpha_q} (1-x)^{\beta_q} \\ &\quad \times f_1(x, \mu_B). \end{aligned} \tag{68}$$

The parameters obtained by fitting to the data in SIDIS processes from HERMES, COMPASS and JLab [11, 15, 17, 20], are listed in Table 1.

In Fig. 2, we depict the QS function  $T_{q,F}(x, x, \mu_B)$  for  $u$  quark,  $d$  quark and  $s$  quark in the proton target as the function of  $x$  at the initial energy scale  $Q_0^2 = 2.4$  GeV<sup>2</sup>, the solid lines correspond to the results from the central values of the parameters, the shaded area shows the uncertainty bands lead by the parameters of Table 1. As one can see from Fig. 2, there are still large errors in the parametrization of the QS function due to the limited amount of the experimental data especially in the case of  $s$  quark QS function. Thus, we emphasis the

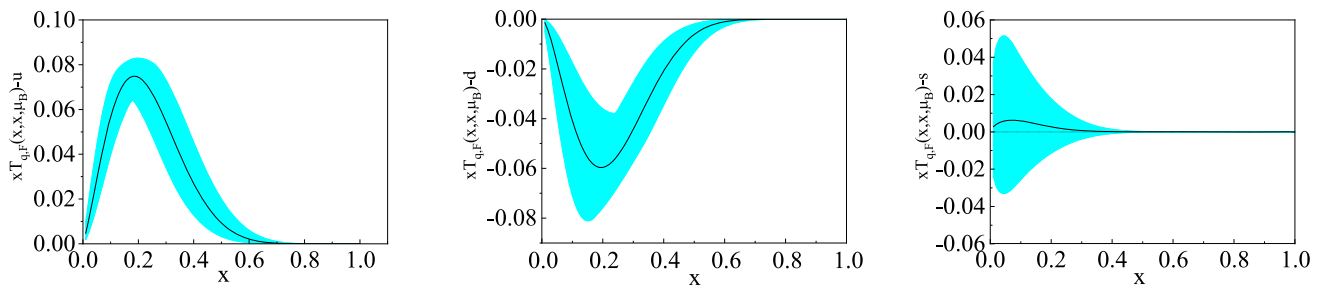


**Fig. 2** The QS function for *u* quark (left panel), *d* quark (middle panel) and *s* quark (right panel). The solid lines correspond to the results from the central values of the parameters, the shaded area shows the uncertainty bands lead by the parameters of Table 1

**Table 1** Values of the parameters in the parameterization of the Qiu-Sterman function in Ref. [32]

Parameter	Value	Parameter	Value
$\alpha_u$	$1.051^{+0.192}_{-0.180}$	$N_{\bar{u}}$	$-0.012^{+0.018}_{-0.020}$
$\alpha_d$	$1.552^{+0.303}_{-0.275}$	$N_{\bar{d}}$	$-0.105^{+0.043}_{-0.060}$
$\alpha_{sea}$	$0.851^{+0.307}_{-0.305}$	$N_s$	$0.103^{+0.548}_{-0.604}$
$\beta$	$4.857^{+1.534}_{-1.395}$	$N_{\bar{s}}$	$-1.000 \pm 1.757$
$N_u$	$0.106^{+0.011}_{-0.009}$	$\langle k_{s\perp}^2 \rangle$	$0.282^{+0.073}_{-0.066} \text{GeV}^2$
$N_d$	$-0.163^{+0.039}_{-0.046}$		

planned electron ion colliders can play an important role in constraining Sivvers function in the future.

We should notice that in Ref. [32], the QS function is assumed to be proportional to the collinear unpolarized distribution function  $f_1(x, \mu_B)$  in which the DGLAP evolution effect is not included. To investigate the impact of the QS function DGLAP evolution effect on the Sivvers asymmetry, we take  $Q_0^2 = 2.4 \text{ GeV}^2$  as the initial energy and evolve the QS function in Eq. (68) into another energy. We adopt two different approaches to evolve the QS function: one is to assume the QS function follows the same evolution effect as that for unpolarized distribution function, the other one is to change the evolution kernel in the QCDNUM evolution package to include the QS evolution kernel by considering the homogenous terms [the terms containing  $T_{q,F}(x, x, \mu_B)$ ] in the evolution kernel as an approximation [91]:

$$P_{qq}^{\text{Sivvers}} \approx \frac{4}{3} \left( \frac{1+z^2}{(1-z)_+} + \frac{3}{2} \delta(1-z) \right) - \frac{3}{2} \frac{1+z^2}{1-z} - 3\delta(1-z). \tag{69}$$

In Eqs. (37) and (38), the free parameter  $g_1$  and the universal parameter  $g_2$  contain information about the evolution of TMDs and are the key parameters that determine the evolution of TMDs from one initial energy  $\mu$  to another  $Q$ . Here we adopt the results given in Ref. [32] for the mean transverse momentum squared  $\langle p_{\perp}^2 \rangle = 0.38 \text{ GeV}^2$  and

$\langle k_{\perp}^2 \rangle = 0.19 \text{ GeV}^2$ . For the universal parameter  $g_2$  in the non-perturbative Sudakov-like form factor, the specific value  $g_2 = 0.16$  is also given in Ref. [32].

The kinematical region that is available at EIC is chosen as follows [52]

$$0.001 < x < 0.4, \quad 0.07 < y < 0.9, \quad 0.2 < z < 0.8, \\ 1 \text{ GeV}^2 < Q^2, \quad W > 5 \text{ GeV}, \\ \sqrt{s} = 100 \text{ GeV}, \quad P_{hT} < 0.5 \text{ GeV}. \tag{70}$$

As for the EicC, the following kinematical cuts are adopted

$$0.005 < x < 0.5, \quad 0.07 < y < 0.9, \quad 0.2 < z < 0.7, \\ 1 \text{ GeV}^2 < Q^2 < 200 \text{ GeV}^2, \\ W > 2 \text{ GeV}, \quad \sqrt{s} = 16.7 \text{ GeV}, \quad P_{hT} < 0.5 \text{ GeV}, \tag{71}$$

where  $W^2 = (P + q)^2 \approx \frac{1-x}{x} Q^2$  is invariant mass of the virtual photon-nucleon system. Since TMD factorization is proved to be valid to describe the physical observables in the region  $P_{hT}/z \ll Q$ ,  $P_{hT}/zQ < 0.5$  is chosen to guarantee the validity of TMD factorization. Combining Eqs. (7), (55) and (65) and the kinematical regions of EIC and EicC, we can calculate the single-spin dependent Sivvers asymmetry of charged Kaon and  $\Lambda$  hyperon produced SIDIS process within the EIC and EicC kinematical region.

The numerical results are shown in Fig. 3. The six rows in the figure depict the results of Sivvers asymmetry of  $K^+$  production,  $K^-$  production, and  $\Lambda$  hyperon production in the EIC and EicC kinematical region, respectively. The predicted experimental observable Sivvers asymmetry are plotted with the statistical error bars (enlarged in the figure), which are estimated as

$$\Delta A = \frac{1}{\sqrt{\mathcal{L}\sigma}}, \tag{72}$$

where  $\sigma$  is the unpolarized cross sections of the corresponding process, and  $\mathcal{L}$  is the integrated luminosity, for which  $\mathcal{L} = 10 \text{ fb}^{-1}$  for EIC and  $50 \text{ fb}^{-1}$  for EicC. The left, central and right panels denote the Sivvers asymmetry as the function

of  $x$ ,  $z$  and  $P_{hT}$ , respectively. In the figure, the black solid line represents the Siverson asymmetry that is obtained when the QS evolution kernel is included to evolve Eq. (68). The red dashed line represents the Siverson asymmetry obtained by using the evolution kernel for the unpolarized distribution function from QCDNUM evolution package to evolve Eq. (68).

As can be seen from Fig. 3, the central values of Siverson asymmetries in the charged Kaon produced and in  $\Lambda$  hyperon produced SIDIS process are sizable in the EIC and EicC kinematical region. Thus, the measurements of the Siverson asymmetry in these facilities provide an ideal tool to obtain the sea quark Siverson function as well as the flavor dependence of the Siverson function. Also, it seems that the magnitude of the asymmetry in EicC is larger than that in EIC. In addition, Fig. 3 shows that the value of the solid line is larger than the dashed line, which indicates that the Siverson asymmetry obtained using the evolution kernel of QS function is greater than that obtained using the unpolarized distribution function evolution kernel. One should note that the DGLAP evolution in the TMD effects may play some role in the future phenomenological analysis of the Siverson asymmetry. Besides, in Fig. 3, the shaded area shows the uncertainty bands of the Siverson asymmetry caused by the parametrization of QS function, which still show large errors. Since we focus on the effect of the QS function on the result, here we don't include the source of uncertainty coming from the DSS parametrization of the collinear unpolarized fragmentation function  $D_1(z)$ .

We can also find from Fig. 3 that the central values of the Siverson asymmetries about  $z$ -dependent and  $P_{hT}$ -dependent in  $K^+$  produced SIDIS process at the kinematical region of EIC and EicC are negative, and the magnitude of the central values of the Siverson asymmetry increases with increasing  $z$  or increasing  $P_{hT}$ . While for the central values of the Siverson asymmetries about  $x$  dependent of  $K^+$  production in the EIC and EicC kinematical region, there is a node around  $x = 0.15$ . On the other hand, for the central values of the Siverson asymmetries of  $K^-$  production, it is always positive in all cases. The central values of the Siverson asymmetry increases with  $x$  at small  $x$  region and decreases along  $x$  at large  $x$  region, and gradually increases with  $z$  and  $P_{hT}$ . In addition, by comparing the magnitudes of the central values of the Siverson asymmetry of  $K^+$  produced with that of  $K^-$  produced, we can see that the former one is larger than the latter one, since for  $K^+$  meson the constituent quarks are  $u$  and  $\bar{s}$ , and for  $K^-$  meson are  $\bar{u}$  and  $s$  quarks. Therefore there is relatively larger contribution of valence  $u$  quark Siverson function for  $K^+$ , while the contributions for  $K^-$  are both from sea quark Siverson function. It is known from Ref. [32] that the QS function of the valence quark is larger than the that of the sea quarks, so the Siverson asymmetry in  $K^+$  produced process is greater than that in  $K^-$  produced process.

In addition, we can clearly see from Fig. 3 that when we consider the uncertainty bands of the QS function, the sign as well as the trend of the asymmetry for  $K^\pm$  production will become blurred. Therefore, it is important that more precise experimental measurements are needed in the future to further constrain the Siverson function. Finally, the central value of Siverson asymmetry for  $\Lambda$  hyperon production in both the EIC and EicC kinematical region is positive, and the tendency of  $x$ ,  $z$  and  $P_{hT}$  dependent asymmetry is generally consistent with that of  $K^-$  meson. In addition, the Siverson asymmetry in  $\Lambda$  hyperon produced process is larger than that in charged Kaon  $K^\pm$  produced process with much smaller uncertainty bands. Thus, the future higher precision EICs may provide a unique opportunity to extract the proton Siverson function of valence quark and sea quark, to investigate the flavor dependence from the  $\Lambda$  hyperon produced SIDIS process, as well as to deeper understand sea quark Siverson function through the analysis with the charged Kaon  $K^+$  production SIDIS process. Combining the experimental data from Drell-Yan process, it may also provide a tool to study the sign change of the Siverson function and the generalized universality of the T-odd distribution functions.

## 4 Conclusion

In this work, we apply the TMD factorization formalism to study the Siverson asymmetry with  $\sin(\phi_h - \phi_s)$  modulation in charged  $K^\pm$  produced and  $\Lambda$  hyperon produced in SIDIS process at the kinematical configurations of EIC and EicC. We take into account the TMD evolution effects of distribution functions as well as fragmentation functions. In our calculation we adopt the Gaussian form parametrization with constant width for the non-perturbative Sudakov-like form factor, the accuracy of the perturbative Sudakov-like form factor as well as the hard coefficients is kept at the NLL order. Two different ways to deal with the energy dependence of Qiu-Sterman function associated with the Siverson function are applied. The first approach is to assume the Qiu-Sterman function evolves as the same way as the unpolarized distribution functions  $f_1(x, Q^2)$ . The second one is to evolve Qiu-Sterman function considering an approximate evolution kernel for the Qiu-Sterman function containing the homogeneous terms by customising the DGLAP kernel. The Siverson asymmetries are calculated as the functions of  $x$ ,  $z$ , and  $P_{hT}$ . Our numerical results demonstrate that the Siverson asymmetries of charged Kaon production and  $\Lambda$  hyperon production are measurable at the kinematics of EIC and EicC, with the magnitudes of around few percents. The results show that the Siverson asymmetry in  $\Lambda$  hyperon production in SIDIS process might serve as a tool to extract the information of sea quark Siverson function as well as to constrain the flavor dependence of Siverson function together with  $K^\pm$  production process by

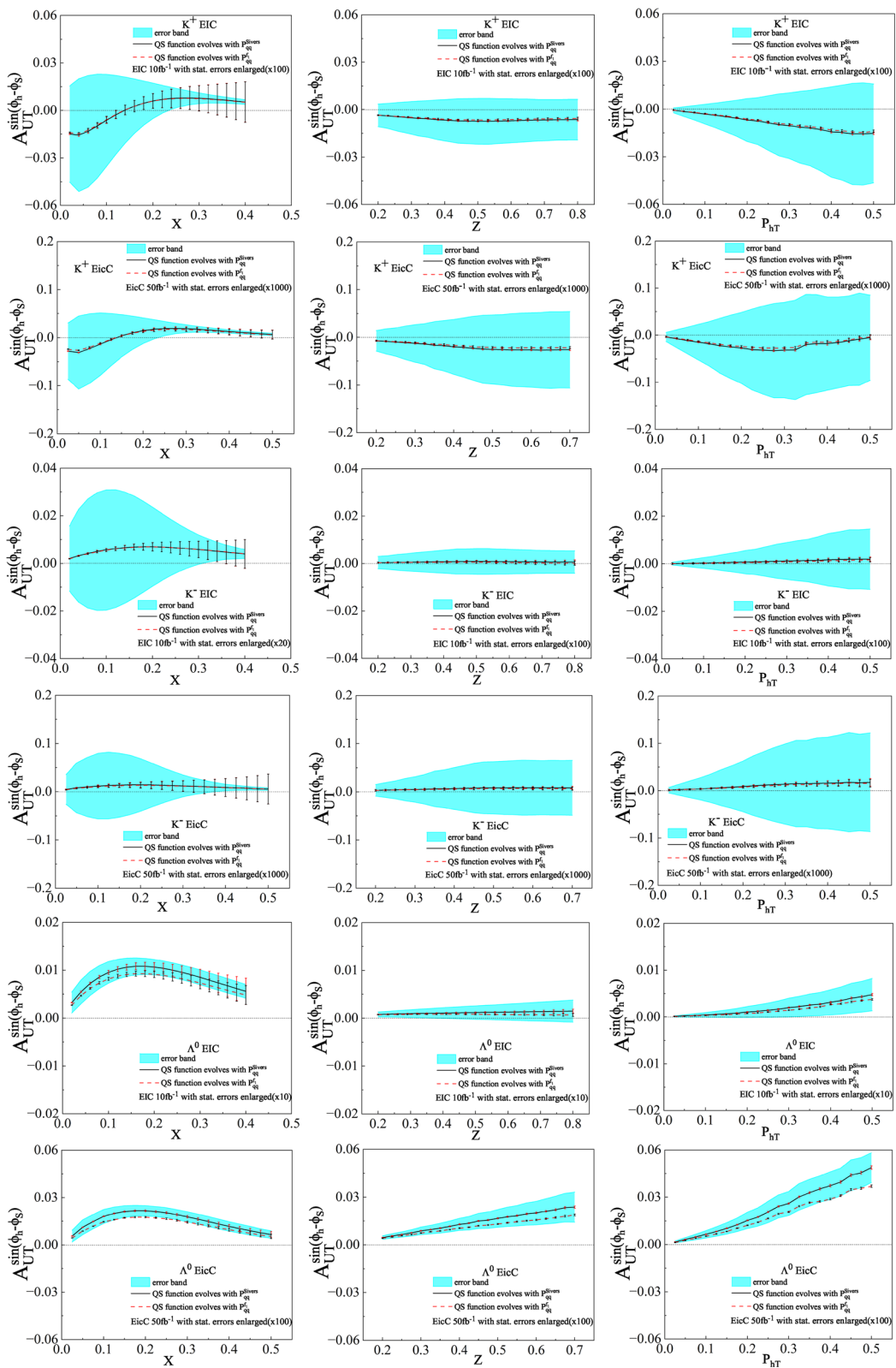


**Fig. 3** The Sivers asymmetry in semi-inclusive charged Kaon and  $\Lambda$  hyperon produced SIDIS process at the kinematics of EIC and EicC as functions of  $x$  (left panels),  $z$  (middle panels), and  $P_{hT}$  (right panels).

The shaded area shows the uncertainty bands of the Sivers asymmetry caused by the parametrization of QS function

utilizing future high energy and high luminosity EICs. In addition, the difference between the Sivers asymmetries from considering two different evolution kernels suggests that the DGLAP evolution of the Qiu–Sterman function in the TMD evolution schemes will play a role in the phenomenological calculation, which should be considered in the future interpretation of experimental data as well as theoretical studies.

**Acknowledgements** This work is partially supported by the NSFC (China) grants 11905187, 11847217 and 12150013. X. Wang is supported by the China Postdoctoral Science Foundation under Grant No. 2018M640680.

**Data availability** This manuscript has no associated data or the data will not be deposited. [Authors' comment: All data generated during this work are contained in the published paper.]

**Open Access** This article is licensed under a Creative Commons Attribution 4.0 International License, which permits use, sharing, adaptation, distribution and reproduction in any medium or format, as long as you give appropriate credit to the original author(s) and the source, provide a link to the Creative Commons licence, and indicate if changes were made. The images or other third party material in this article are included in the article's Creative Commons licence, unless indicated otherwise in a credit line to the material. If material is not included in the article's Creative Commons licence and your intended use is not permitted by statutory regulation or exceeds the permitted use, you will need to obtain permission directly from the copyright holder. To view a copy of this licence, visit <http://creativecommons.org/licenses/by/4.0/>.

Funded by SCOAP<sup>3</sup>. SCOAP<sup>3</sup> supports the goals of the International Year of Basic Sciences for Sustainable Development.

## References

1. J. Ashman et al. (European Muon), Phys. Lett. B **206**, 364 (1988)
2. J. Ashman et al. (European Muon), Nucl. Phys. B **328**, 1 (1989)
3. D.W. Sivers, Phys. Rev. D **41**, 83 (1990)
4. D.W. Sivers, Phys. Rev. D **43**, 261 (1991)
5. J.C. Collins, Nucl. Phys. B **396**, 161 (1993)
6. S.J. Brodsky, D.S. Hwang, I. Schmidt, Phys. Lett. B **530**, 99 (2002)
7. S.J. Brodsky, D.S. Hwang, I. Schmidt, Nucl. Phys. B **642**, 344 (2002)
8. D. Boer, S.J. Brodsky, D.S. Hwang, Phys. Rev. D **67**, 054003 (2003)
9. J.C. Collins, Phys. Lett. B **536**, 43 (2002)
10. A. Airapetian et al. (HERMES), Phys. Rev. Lett. **94**, 012002 (2005)
11. A. Airapetian et al. (HERMES), Phys. Rev. Lett. **103**, 152002 (2009)
12. A. Airapetian et al. (HERMES), J. High Energy Phys. **12**, 010 (2020)
13. V.Y. Alexakhin et al. (COMPASS), Phys. Rev. Lett. **94**, 202002 (2005)
14. E.S. Ageev et al. (COMPASS), Nucl. Phys. B **765**, 31 (2007)
15. M. Alekseev et al. (COMPASS), Phys. Lett. B **673**, 127 (2009)
16. M.G. Alekseev et al. (COMPASS), Phys. Lett. B **692**, 240 (2010)
17. C. Adolph et al. (COMPASS), Phys. Lett. B **717**, 383 (2012)
18. C. Adolph et al. (COMPASS), Phys. Lett. B **770**, 138 (2017)
19. M.G. Alexeev et al. (COMPASS), Nucl. Phys. B **940**, 34 (2019)
20. X. Qian et al. (Jefferson Lab Hall A), Phys. Rev. Lett. **107**, 072003 (2011)
21. Y.X. Zhao et al. (Jefferson Lab Hall A), Phys. Rev. C **90**, 055201 (2014)
22. M. Aghasyan et al. (COMPASS), Phys. Rev. Lett. **119**, 112002 (2017)
23. C.A. Aidala et al., (2019). [arXiv:1901.08002](https://arxiv.org/abs/1901.08002)
24. L. Adamczyk et al. (STAR), Phys. Rev. Lett. **116**, 132301 (2016)
25. M. Anselmino, M. Boglione, U. D'Alesio, A. Kotzinian, F. Murgia, A. Prokudin, Phys. Rev. D **72**, 094007 (2005). [Erratum: Phys. Rev. D **72**, 099903 (2005)]
26. A.V. Efremov, K. Goeke, S. Menzel, A. Metz, P. Schweitzer, Phys. Lett. B **612**, 233 (2005)
27. J.C. Collins, A.V. Efremov, K. Goeke, S. Menzel, A. Metz, P. Schweitzer, Phys. Rev. D **73**, 014021 (2006)
28. W. Vogelsang, F. Yuan, Phys. Rev. D **72**, 054028 (2005)
29. M. Anselmino, M. Boglione, U. D'Alesio, A. Kotzinian, S. Melis, F. Murgia, A. Prokudin, C. Turk, Eur. Phys. J. A **39**, 89 (2009)
30. M. Anselmino, M. Boglione, S. Melis, Phys. Rev. D **86**, 014028 (2012)
31. A. Bacchetta, M. Radici, Phys. Rev. Lett. **107**, 212001 (2011)
32. M.G. Echevarria, A. Idilbi, Z.-B. Kang, I. Vitev, Phys. Rev. D **89**, 074013 (2014)
33. M. Anselmino, M. Boglione, U. D'Alesio, F. Murgia, A. Prokudin, J. High Energy Phys. **04**, 046 (2017)
34. A. Martin, F. Bradamante, V. Barone, Phys. Rev. D **95**, 094024 (2017)
35. M. Boglione, U. D'Alesio, C. Flore, J.O. Gonzalez-Hernandez, J. High Energy Phys. **07**, 148 (2018)
36. M. Bury, A. Prokudin, A. Vladimirov, J. High Energy Phys. **05**, 151 (2021)
37. A. Bacchetta, F. Delcarro, C. Pisano, M. Radici, Phys. Lett. B **827**, 136961 (2022)
38. A. Bacchetta, A. Schaefer, J.-J. Yang, Phys. Lett. B **578**, 109 (2004)
39. A. Bacchetta, F. Conti, M. Radici, Phys. Rev. D **78**, 074010 (2008)
40. Z. Lu, B.-Q. Ma, Phys. Rev. D **70**, 094044 (2004)
41. B. Pasquini, F. Yuan, Phys. Rev. D **81**, 114013 (2010)
42. T. Maji, D. Chakrabarti, A. Mukherjee, Phys. Rev. D **97**, 014016 (2018)
43. T. Maji, D. Chakrabarti, O.V. Teryaev, Phys. Rev. D **96**, 114023 (2017)
44. A. Courtoy, F. Fratini, S. Scopetta, V. Vento, Phys. Rev. D **78**, 034002 (2008)
45. F. Yuan, Phys. Lett. B **575**, 45 (2003)
46. A. Courtoy, S. Scopetta, V. Vento, Phys. Rev. D **79**, 074001 (2009)
47. V.E. Lyubovitskij, I. Schmidt, S.J. Brodsky, Phys. Rev. D **105**, 114032 (2022)
48. H. Dong, D.-X. Zheng, J. Zhou, Phys. Lett. B **788**, 401 (2019)
49. F. He, P. Wang, Phys. Rev. D **100**, 074032 (2019)
50. X. Luan, Z. Lu, Phys. Lett. B **833**, 137299 (2022)
51. D. Boer, M. Diehl, R. Milner, R. Venugopalan, W. Vogelsang, A. Accardi, E. Aschenauer, M. Burkardt, R. Ent, V. Guzey, et al., (2011). [arXiv:1108.1713](https://arxiv.org/abs/1108.1713)
52. A. Accardi et al., Eur. Phys. J. A **52**, 268 (2016)
53. R. Abdul Khalek et al., Nucl. Phys. A **1026**, 122447 (2022)
54. X. Cao, X. Chen, L. Gui, C. Han, L. Kaptari, M. Li, Y. Liang, L. Liu, F. Ma, L. Mao et al., He Jishu **43**, 020001 (2020)
55. D.P. Anderle et al., Front. Phys. (Beijing) **16**, 64701 (2021)
56. J. C. Collins, D. E. Soper, Nucl. Phys. B **193**, 381 (1981). [Erratum: Nucl. Phys. B **213**, 545 (1983)]
57. J.C. Collins, D.E. Soper, G.F. Sterman, Nucl. Phys. B **250**, 199 (1985)
58. J. Collins, Foundations of perturbative QCD, vol. 32 (Cambridge University Press, 2013) (ISBN 978-1-107-64525-7, 978-1-107-64525-7, 978-0-521-85533-4, 978-1-139-09782-6)
59. X.-D. Ji, J.-P. Ma, F. Yuan, Phys. Lett. B **597**, 299 (2004)
60. X.-D. Ji, J.-P. Ma, F. Yuan, Phys. Rev. D **71**, 034005 (2005)
61. S.M. Aybat, T.C. Rogers, Phys. Rev. D **83**, 114042 (2011)
62. J.C. Collins, T.C. Rogers, Phys. Rev. D **87**, 034018 (2013)

63. M.G. Echevarria, A. Idilbi, A. Schäfer, I. Scimemi, *Eur. Phys. J. C* **73**, 2636 (2013)
64. A. Bacchetta, F. Delcarro, C. Pisano, M. Radici, A. Signori, *JHEP* **06**, 081 (2017). [Erratum: *JHEP* **06**, 051 (2019)]
65. I. Scimemi, A. Vladimirov, *JHEP* **06**, 137 (2020)
66. A. Bacchetta, V. Bertone, C. Bissolotti, G. Bozzi, M. Cerutti, F. Piacenza, M. Radici, A. Signori (MAP Collaboration), *JHEP* **10**, 127 (2022)
67. D. Pitonyak, M. Schlegel, A. Metz, *Phys. Rev. D* **89**, 054032 (2014)
68. D. Boer, *Nucl. Phys. B* **806**, 23 (2009)
69. S. Arnold, A. Metz, M. Schlegel, *Phys. Rev. D* **79**, 034005 (2009)
70. A. Bacchetta, V. Bertone, C. Bissolotti, G. Bozzi, F. Delcarro, F. Piacenza, M. Radici, *JHEP* **07**, 117 (2020)
71. M. Lambertsen, W. Vogelsang, *Phys. Rev. D* **93**, 114013 (2016)
72. J.C. Collins, F. Hautmann, *Phys. Lett. B* **472**, 129 (2000)
73. A. Bacchetta, U. D'Alesio, M. Diehl, C.A. Miller, *Phys. Rev. D* **70**, 117504 (2004)
74. A. Bacchetta, M. Diehl, K. Goeke, A. Metz, P.J. Mulders, M. Schlegel, *JHEP* **02**, 093 (2007)
75. A. Idilbi, X.-D. Ji, J.-P. Ma, F. Yuan, *Phys. Rev. D* **70**, 074021 (2004)
76. A. Bacchetta, A. Prokudin, *Nucl. Phys. B* **875**, 536 (2013)
77. Z.-B. Kang, B.-W. Xiao, F. Yuan, *Phys. Rev. Lett.* **107**, 152002 (2011)
78. S.M. Aybat, J.C. Collins, J.-W. Qiu, T.C. Rogers, *Phys. Rev. D* **85**, 034043 (2012)
79. M.G. Echevarria, A. Idilbi, I. Scimemi, *Phys. Rev. D* **90**, 014003 (2014)
80. F. Landry, R. Brock, P.M. Nadolsky, C.P. Yuan, *Phys. Rev. D* **67**, 073016 (2003)
81. J.-W. Qiu, X.-F. Zhang, *Phys. Rev. Lett.* **86**, 2724 (2001)
82. A.V. Konychev, P.M. Nadolsky, *Phys. Lett. B* **633**, 710 (2006)
83. C.T.H. Davies, B.R. Webber, W.J. Stirling, **1**, I.95 (1984)
84. R.K. Ellis, D.A. Ross, S. Veseli, *Nucl. Phys. B* **503**, 309 (1997)
85. Z.-B. Kang, A. Prokudin, P. Sun, F. Yuan, *Phys. Rev. D* **93**, 014009 (2016)
86. P. Sun, F. Yuan, *Phys. Rev. D* **88**, 114012 (2013)
87. A.D. Martin, W.J. Stirling, R.S. Thorne, G. Watt, *Eur. Phys. J. C* **63**, 189 (2009)
88. D. de Florian, R. Sassot, M. Stratmann, *Phys. Rev. D* **75**, 114010 (2007)
89. Y. Yang, Z. Lu, I. Schmidt, *Phys. Rev. D* **96**, 034010 (2017)
90. M. Botje, *Comput. Phys. Commun.* **182**, 490 (2011)
91. Z.-B. Kang, J.-W. Qiu, *Phys. Rev. D* **79**, 016003 (2009)